

Published in final edited form as:

J Arthroplasty. 2013 September ; 28(8): . doi:10.1016/j.arth.2012.11.020.

Preclinical Evaluation of a Novel Implant for Treatment of a Full-Thickness Distal Femoral Focal Cartilage Defect

Erik I. Waldorff, PhD^a, Blake J. Roessler, MD^b, Terri A. Zachos, DVM, PhD^c, Bruce S. Miller, MD, MS^a, Jonathan McHugh, MD^d, and Steven A. Goldstein, PhD^a

^a Orthopaedic Research Laboratories, Department of Orthopaedic Surgery, University of Michigan, Ann Arbor, Michigan

^b Department of Internal Medicine, Rheumatology, University of Michigan, Ann Arbor, Michigan

^c College of Human Medicine, Michigan State University, Kalamazoo, Michigan

^d Department of Pathology, University of Michigan, Ann Arbor, Michigan

Abstract

A novel, nonresorbable, monolithic composite structure ceramic, developed using a partially stabilized zirconia ceramic common to implantable devices, was used in a cementless weight-bearing articular implant to test the feasibility of replacing a region of degenerated or damaged articular cartilage in the knee as part of a preclinical study using male mongrel dogs lasting up to 24 weeks. Gross/histological cartilage observations showed no differences among control, 12-week and 24-week groups, while pull-out tests showed an increase in maximum pull-out load over time relative to controls. Hence, the use of a novel ceramic implant as a replacement for a focal cartilage defect leads to effective implant fixation within 12 weeks and does not cause significant degradation in opposing articular cartilage in the time frame evaluated.

Keywords

unicondylar hemiarthroplasty; ceramic device; preclinical study; cartilage wear; animal model

Full-thickness focal cartilage defects in the femoral condyle can occur as a result of normal aging [1,2] or trauma [3–6]. If severe enough, they can be painful and debilitating [6]. Evidence of these lesions is well documented in clinical literature [7]. Left untreated, focal cartilage defects can disrupt the continuous articular surface and potentially lead to osteoarthritis [6,8].

In cases of severe osteoarthritis, a total knee arthroplasty (TKA) is usually the most effective therapeutic solution [9]. TKA works well, but is limited by wear and loosening, resulting in the need for revision surgery within 15–20 years [10–14]. For younger TKA patients (35–50 years old), revision surgery is even more likely, because the increased activity of these younger patients leads to more implant wear and a reduced lifespan of the first TKA [15–17], although more recent follow-ups have shown some improvements in TKA lifespan [18,19]. Revision surgery often leads to poor outcomes due to bone loss associated with the removal of the initial device and impairment of wound vascularity [13,16,20–23]. Since the

© 2013 Elsevier Inc. All rights reserved.

Reprint requests: Steven A. Goldstein, PhD, Orthopaedic Research, Laboratories, Department of Orthopaedic Surgery, University of Michigan, 2003 BSRB, 109, Zina Pitcher Place, Ann Arbor, MI 48109.

The Conflict of Interest statement associated with this article can be found at <http://dx.doi.org/10.1016/j.arth.2012.11.020>.

potential complications with revision TKAs are significant, primary TKAs are frequently delayed until the risks for revision are reduced [24]. Theoretically, this could be done by procedures or devices developed to restore functional and pain-free patient mobility along with a reduction in further degradation of the surrounding cartilage.

Several methods designed to address these issues are available. Microfracture has shown acceptable results [25]. However, the resulting collagen surface is mainly composed of collagen type I, which deteriorates significantly within 18 months [26]. In addition, the integrity of the underlying subchondral bone might still be compromised, which may result in poor outcomes. Autografts are expensive, involve a lengthy procedure with possible donor-site morbidity and are not always successful [27,28], while allografts have the added risk of possible immune-based rejection [29]. Autologous chondrocyte grafting has had good outcomes [30,31], but as with autografts, the procedure is lengthy and expensive with possible donor-site morbidity. In addition, the procedure faces limitations of available cartilage and possible differences in orientation and properties between donor and recipient cartilage [29,30,32]. Tissue-engineered cartilage has shown only moderate progress and does not always have successful outcomes [33]. Autologous chondrocyte implantation has also shown some success [31], but is expensive and has shown joint space narrowing following surgery, a need for re-operation for debridement, periosteal hypertrophy, partial patch delamination and graft failures [31].

Finally, focal hemiarthroplasty is also available. Based on reconstructive device concepts, previous investigations of focal hemiarthroplasties have explored the use of a variety of materials ranging from alloys [34,35] to polymer composites [36]. Current research into this device concept continues to demonstrate potential benefits [37]. However, the substantial mismatches in modulus between native subchondral bone and implant materials may create potential limitations relating to biologic fixation and stress shielding.

Investigations on porous-coated implant topology [38] led to the development of a novel nonresorbable articular matrix ceramic which was used to test the feasibility of replacing a region of degenerated or damaged cartilage in a preclinical large-animal model. Two primary hypotheses were tested: (1) The use of a ceramic articulation surface, as part of a regional replacement of cartilage, has no damaging effects on native articular cartilage after 24 weeks; and (2) a composite ceramic implant with a macroscopically porous topology and conical geometry can provide immediate fixation and promote secure long-term bone adaptation.

Materials and Methods

Ceramic Device

The device (Fig. 1) used in this study consisted of a nonresorbable monolithic composite structure ceramic, developed using partially stabilized zirconia (PSZ) ceramic common to existing implantable devices. A weight-bearing cementless articular implant was designed using this material for implantation into the distal medial femoral condyle (knee) of the study animals. High-resolution computed tomography scan data of the experimental animal knee joint were transferred into a computed-aided design platform (Pro/ENGINEER, PTC-Needham, MA) to provide surface data for defining the curvature of the articular surface of the implant along with distal femoral bone volume data to position the fixation cones. The implant has a highly polished submicron articular surface integrated with a porous ingrowth structure consisting of interconnected porosity N50%, with a pore-size distribution similar to those used in porous metal devices [39]. The device design is similar to that of an osteochondral graft. The articular surface has an oval foot print 13.5 mm in length and 8.4 mm in width, with two 6.4-mm-long porous cones protruding from the base (Fig. 1). Based

on previous studies [38], the cones are tapered to provide a wide range of stresses to the underlying trabecular bone tissue, in an effort to optimize cementless fixation.

Experimental Design

Fifteen (15) large male adult mongrel dogs were used in the study (31.9 kg±4.7 kg). This animal model was selected to compare cone ingrowth with that of a previous model [38]. The animals were assigned to the following groups: unoperated controls (UC; n=2); controls, day 0 (n=3); 12 weeks postsurgery (n=3); 24 weeks postsurgery (n=7). Following euthanization of the animals, the tibial plateau and medial femoral condyle were assigned to histological examinations, biomechanical pull-out tests or x-ray diffraction (XRD) examination (Fig. 2). This work was approved by our institution's Committee on Use and Care of Animals.

Surgical Procedure

Animals assigned to the experimental groups underwent bilateral implantation of the ceramic device. Specifically, under completely sterile conditions, using a minimally invasive approach, a small incision was made on the medial aspect of the knee from just distal of the patella to the center of the patella. With the knee in full extension the fat pad, just distal to the femoral condyles, was removed while ensuring preservation of the meniscus. With the knee in full flexion the medial condyle of the distal femur could now be exposed. For a few early animals (two control, one 12-week, and two 24-week), a para-patella, more invasive approach was used, including dislocation of the patella, prior to removing the fat pad. After exposure, articular cartilage and underlying subchondral bone of the region of interest on the medial femoral condyle were removed using a series of custom guides and drills to produce a defect that exactly matched the footprint of the implant and shape of the implant cones (Fig. 3A). The implant was then press-fit by hand into the excavated region, while ensuring that the articular surface was flush with the remaining native articular cartilage (Fig. 3B). After soft tissue closure with resorbable sutures and skin staples, postoperative radiographs were taken to verify placement of the implant. The animals were allowed full weight-bearing and normal cage activity immediately following surgery.

Radiographs

In addition to the immediate postoperative radiographs, radiographs were taken weekly for the first month, biweekly for the following two months, and finally monthly. These radiographs were taken to ensure that no loosening of the device had occurred and to reconfirm good overall placement of the implant and congruous alignment of the implant articular surface with the surrounding native cartilage surface (Fig. 3C).

Animal Exercise and Observation

In addition to free cage activity (cage foot print: 8'×8'), each dog was allowed 30 min/day for free roaming in a larger area. During this time animals were observed for lameness of their hindlimbs.

Gross Cartilage Evaluation

Upon dissection of all hindlimbs, high-resolution digital images were taken of the articular cartilage of the medial/lateral tibial/femoral articular surfaces. Using these images the articular cartilage was scored by two independent reviewers using the Collins score [40]. The average of the two readings per specimens was used as the representative Collins score for each specimen. The group sizes used for the statistical comparison for gross cartilage evaluation were as follows: UC, n=4; controls, day 0, n=6; 12 weeks postsurgery, n= 6; 24

weeks postsurgery, n=12. These group sizes were achieved due to specimens being taken from both legs for each animal.

Histology

The hindlimbs assigned to histology were fixed in 10% NBF and subsequently stored in 70% ETOH until further processing.

Tibial Articular Cartilage Evaluation (Safranin O)

The tibial plateaus of the hindlimbs destined for histology were decalcified in 5% formic acid for ~40 days, embedded in paraffin, and sectioned transverse to the anterior–posterior (AP) axis (7 μ m thick). Two sections (located \pm 1.4 mm relative to the center) within each tibial plateau (medial and lateral) were stained with Safranin O for cartilage evaluation. Two independent and blinded reviewers examined the sections using light microscopy and scored the articular cartilage using the 14-point Mankin score [41,42]. The average score of the two sections within each specific plateau is presented in the Results section below. In addition, the stain intensity was quantified using light microscopy (1.6 \times magnification) and ImageJ (1.42q, National Institutes of Health, USA) for three locations within each section: the top, middle and bottom third of the cartilage thickness (articular edge to subchondral bone; Fig. 4). Within each animal, the intensities were normalized to the intensity of the bottom 1/3 of the lateral tibial plateau (set to 100). The average intensity within each similar location of the two sections is presented in the Results. The group sizes used for statistical comparison for the Mankin scoring and ImageJ analysis were as follows: UC, n=2; controls, day 0, n=3; 12 weeks postsurgery, n=3; 24 weeks postsurgery, n=6.

Cartilage Implant Overgrowth (Toluidine Blue)

The histology-assigned medial femoral condyles containing the implants were embedded in PMMA and sectioned along the AP axis (300 μ m thick) through the width of the implant using an Exakt diamond blade saw. The center section of the implant was mounted on a plastic microscope slide using cyanoacrylate and polished to a final thickness of 150–200 μ m. The sections were etched using 0.1% formic acid and subsequently stained with 1% Toluidine Blue. Because cartilage overgrowth was expected on the implant, overgrowth was determined too. Specifically, using light microscopy at 4 \times magnification, the implant articular surface length (IASL) and the percent IASL covered by cartilage were calculated with Bioquant image software (BQ OSTEO v.7.20.10). The group sizes used for the statistical comparison for cartilage implant overgrowth analysis were as follows: controls, day 0, n = 3; 12 weeks postsurgery, n = 3; 24 weeks postsurgery, n=6.

Bone Apposition and Implant Bone Ingrowth (SEM)

The opposing PMMA-embedded center section relative to the Toluidine Blue stained section was also mounted on a plastic microscope slide using cyanoacrylate and polished to a final thickness of 150–200 μ m. The section was carbon coated for scanning electron microscopy (SEM) analysis of bone apposition and ingrowth into the implant cones. Images taken at 7.5–8.5 \times magnification were analyzed using ImageJ to determine bone apposition and bone ingrowth parameters (Fig. 5). Specifically, bone apposition was determined for a region of interest ranging from the cone surface to 200 μ m parallel to it. Both sides of each cone were examined, resulting in four apposition regions for each section. The average for all apposition regions is presented. The average percent bone ingrowth within the void of each cone was calculated, and the average ingrowth into the two cones for each implant is presented. The group sizes used for statistical comparison for the bone apposition and implant bone ingrowth analysis were as follows: controls, day 0, n=3; 12 weeks postsurgery, n=3; 24 weeks postsurgery, n=6.

Biomechanical Pull-Out Test

The diaphyses of the femurs assigned for pull-out tests were cut through transverse to the long axis, and 5 inches from the distal end. The remaining distal portion of the femur (containing the implant) was embedded in PMMA, and the cartilage immediately medial and lateral to the implant was removed using a drill shaping tool (Dremmel; Fig. 6A) to ensure that a custom clamp could be situated underneath the implant articular ridge. A multidirectional vice (Fig. 6B) was used to vertically align the specimen in a servohydraulic testing machine (858 Mini Bionix II, MTS System, Eden Prairie, MN) for a unidirectional tensile pull-out test. The displacement of the loading head was monitored using the MTS internal LVDT, while load was recorded using a 500-lb load cell (Sensotec, Columbus, OH) in series with the actuator. Using the Test Star IIs system (version 2.4, MTS, Eden Prairie, MN), load and displacement were recorded at a sampling rate of 40 Hz, while the pull-out test was performed at a rate of 1 mm/min for 5 min. The ultimate load was calculated from the load–displacement curves using MATLAB (The Mathworks Inc., Natick, MA). The group sizes used for statistical comparison for the biomechanical pull-out tests were as follows: controls, day 0, n=3; 12 weeks postsurgery, n=3; 24 weeks postsurgery, n=5.

Evaluation for Material Stability of the Ceramic

Upon completion of the mechanical pull-out test, an implant from each group was randomly selected and evaluated for material phase stability following exposure to the biologic environment. The explants were evaluated by determining the percent of monoclinic phase present in the fully dense articular region and in the porous region of the ceramic. This was done using XRD with a low grazing angle [43] and calculated using the ratio of integrated peak areas [44]. Nonimplanted specimens were also evaluated. All specimens (implanted and nonimplanted) were analyzed on two sides; the highly polished, articular surface and the porous bone ingrowth matrix (scaffold) in the areas of failure following pull-out testing.

Statistical Methods

A Student's t-test was used for comparisons between groups (unpaired) and across times (paired). A Pearson's Correlation was calculated where appropriate. All analyses were performed using SPSS statistical software (SPSS, Chicago, IL). Significance (*) was defined as $P < .05$. Data are presented as average \pm standard deviation.

Results

The animals appeared fully weight bearing within 2 h of surgery. However, due to a lax patella related to the surgical exposure, one animal from the 24-week group had to be euthanized at week 4. All other animals showed no lameness to their hindlimbs following surgery for the entire duration of the experiment. The data from the animal euthanized at week 4 have been included to provide a view of an additional intermediate time point. Due to the singularity of this time point no statistical comparisons have been made in relation to it.

Review of postoperative radiographs revealed that all implants had good overall placement and congruous alignment of the implant articular surface with the surrounding cartilage surface. In addition the radiographs showed no loosening of the implant for any animals at any time point. Finally, no degenerative changes of the opposing cartilage (at the tibial plateau) were observable on the radiographs at any time points.

Gross cartilage observation showed no differences in Collins cartilage score among any groups for the lateral tibial plateau (Fig. 7). For the medial tibial plateau no differences were

found among the control, 12-week and 24-week groups (Fig. 7). However, the UC group had a lower score compared to all other groups.

Evaluation of the articular cartilage of the tibial plateau using the Mankin score for sections stained with Safranin O revealed a higher score for the lateral region for the 12- and 24-week groups relative to the UC group (Fig. 8). The lateral region for the 24-week group was also higher compared to the control group. In addition, it was found that the medial region for the control and 24-week groups was higher relative to the UC group. No differences were found between the lateral and medial regions for any groups except the control group (Fig. 8).

Results from the Safranin O intensity measurements indicate that the top third of the cartilage (region 1) had a lower intensity than both the middle and bottom for both the medial (control, 12-week, 24-week) and lateral tibial plateaus (control, UC, 12-week, 24-week; Figs. 9A and B). For the medial plateau no differences were found among any groups when comparing similar regions (Fig. 9A). For the lateral plateau it was found that region 1 for the UC and 12-week groups was higher relative to the control group (Fig. 9B). No differences were found in intensity within similar regions between the lateral and medial plateaus for any groups.

Toluidine Blue staining showed significant cartilage overgrowth (mostly fibro-cartilaginous) upon the implant over time (Fig. 10).

SEM examinations showed a significant increase in bone apposition (Fig. 11A) and overall bone ingrowth over time (Fig. 11B).

Pull-out tests showed an increase in maximum load at pull-out for the 12-week group relative to the control group (Fig. 12). Although not significant, a trend of an increase ($P=$.10) was found for the 24-week group relative to the control group (Fig. 12).

All specimens that underwent XRD showed a percent monoclinic phase of <3% for both the articular and scaffold surface (Table 1), which was similar to nonimplanted specimens and significantly below the 25% threshold outlined in the ISO standard for the material [44].

Discussion

We have found that the use of a novel ceramic implant as a replacement for a focal cartilage defect leads to secure implant fixation, while not causing significant degradation in opposing articular cartilage.

Within hours of surgical implantation animals were fully ambulating with no changes in the function of their hindlimbs. For the duration of the experiment no lameness to their hindlimbs was observed, indicating that immediate mobilization of the treated limb is possible with the minimally invasive press-fit implantation of the device.

In addition, the possibility for early weight bearing is supported by the postoperative radiographs that indicated that no loosening of the implants had taken place, thereby enabling faster healing and return to play.

Although the surgical procedure required the manual application of a series of custom guides to produce the desired excavated footprint for the implant, the tolerances and techniques were precise enough to enable a firm press fit of the porous cones extending from the implant. The press-fit implantation of the device was shown to be secure enough for normal activity immediately following surgery until adequate bone apposition and ingrowth had occurred. SEM and biomechanical test results indicate that this happened within 12

weeks, at which time the novel porous cone design had led to complete implant fixation. Despite significant ingrowth, the lower pull-out strength for the 24-week group relative to the 12-week group occurred from failure at the base of the cones during testing in two specimens. Further investigation of this failure mode seems to indicate that the ingrown cones exhibit strength greater than the tensile strength of the porous ceramic. It should be noted that this testing technique was used to help define bone ingrowth and not to characterize the mechanical strength of the material. The specific characterization of this material for implant use was conducted prior to this animal study by the sponsor and determined to be adequate for the device application. Biomechanically, tensile loads would be expected to be relatively low in vivo, given that compressive loads and possibly shear loads dominate during normal gait activities. An argument could be made that distinguishable asymmetry related to the ingrowth of the independent cones, i.e., one displaying significantly less ingrowth or becoming loose relative to the other, could cause a tensile condition, but this condition did not appear with any implant evaluated in this study. Most pull-out failures occurred at the tip of the cones, effectively measuring the specific bone/cone interface. Despite the potential for tensile failure, the cones were found to be structurally sound enough to maintain implant placement and the integrity of a continuous articular surface throughout the study. In light of this finding, however, future device design improvements using this material are being developed.

The XRD measurements for percent monoclinic showed very low levels of phase transformation over the test period. These results suggest stability of the ceramic material against aging due to low-temperature degradation for this application.

Although cartilage coverage of the articular surface of the implant increased significantly over time, the characteristics were mostly fibro-cartilaginous in nature, which is similar to what has been seen with other cartilage replacement devices [34,35]. Although not of similar material properties as native articular cartilage, the coverage seems to help create a smooth transition from the healthy cartilage to the polished articular surface of the implant. The coverage of the implant with fibro-cartilage is similar to what has been observed with cartilage plugs where a 'flow' of cartilage surrounding the defect occurs [45]. Despite the nonindigenous nature of the 'flowing' cartilage at the articular surface, it can be argued that the increased cartilage coverage does not have a detrimental effect on the opposing cartilage on the tibial plateau based on the Safranin O intensity results presented (Fig. 9). However, correlations were observed between percent implant articular surface length covered by cartilage and gross Collins score of the medial tibial plateau (Pearson's correlation: 0.241, $P=.427$), Mankin score of the medial tibial plateau (Pearson's correlation: 0.355, $P=.235$), and Safranin O intensity of Region 1 (outer layer) of the medial tibial plateau (Pearson's correlation: 0.104, $P=.734$). These correlations, however, were weak and statistically non-significant. Hence, fibro-cartilage overgrowth might play a role with some degeneration but in the time frame presented here this degeneration does not become significant. Finally the preservation of healthy hyaline cartilage surrounding the implant supports the usage of a ceramic over a cartilage plug, where localized 'flow' of fibro-cartilage over the plug has been shown to lead to plug degeneration and frayed surrounding cartilage for both deep and superficial defects [46,47].

The lower Collins and Mankin scores in the UC group relative to the other groups seem to be due to surgical exposure of the cartilage, as reflected in the similar results between the control and 12/24-week groups. This observation is supported by studies that have shown histochemical and ultrastructural changes in articular cartilage immediately following surgery [48,49]. In addition, since no changes were seen for the Mankin scoring and the Safranin O intensity measurements between the lateral and medial plateaus, one can assume that the degenerative changes caused by the implant itself are nonsignificant up to 24 weeks.

However, sacrificing animals at later time points could potentially reveal significant changes not observed within the examined time frame.

This study does have limitations. Despite using contra lateral limbs and within-limb controls (Fig. 2), group size could potentially be too small for nonsignificance to be accurately measured for the Safranin O outcome measures. However, the significantly larger group sizes used for the cross-cartilage measures revealed results that paralleled the Safranin O results, thus supporting the overall conclusion. In addition, the potentially small-sized groups do not negate the validity of the significant findings for several key measures. This includes the significant increase in pull-out strength paralleled by the significant increase in bone ingrowth over time measured with SEM. Another limitation is the duration that animals were kept with the implant. Twenty-four weeks is a medium-sized timeframe that gives a good estimation of the initial cartilage and bone response to the implantation of the ceramic as an articular surface. However longer term projections are desired and will be used in a subsequent study.

In summary, the use of a ceramic implant appears to be an effective, secure focal cartilage replacement up to 24 weeks that may increase the therapeutic options for focal cartilage lesions. Further studies are needed to determine any long-term effects beyond 24 weeks.

Acknowledgments

The authors thank Jeff Gordon, Paul Johnson and Ken Johannaber (all from Synvasive Technology Inc., Reno, NV) for their advice concerning experimental setup and for evaluation of the material phase stability using XRD.

References

1. Temple MM, Bae WC, Chen MQ, et al. Age- and site-associated biomechanical weakening of human articular cartilage of the femoral condyle. *Osteoarthritis Cartilage*. 2007; 15(9):1042. [PubMed: 17468016]
2. Bendele AM, Hulman JF. Spontaneous cartilage degeneration in guinea pigs. *Arthritis Rheum*. 1988; 31(4):561. [PubMed: 3358814]
3. Wegrzyn J, Chouteau J, Philippot R, et al. Repeat revision of anterior cruciate ligament reconstruction: a retrospective review of management and outcome of 10 patients with an average 3-year follow-up. *Am J Sports Med*. 2009; 37(4):776. [PubMed: 19336620]
4. Hjelle K, Solheim E, Strand T, et al. Articular cartilage defects in 1,000 knee arthroscopies. *Arthroscopy*. 2002; 18(7):730. [PubMed: 12209430]
5. Pinczewski LA, Deehan DJ, Salmon LJ, et al. A five-year comparison of patellar tendon versus four-strand hamstring tendon autograft for arthroscopic reconstruction of the anterior cruciate ligament. *Am J Sports Med*. 2002; 30(4):523. [PubMed: 12130407]
6. Onstott AT, Moczko A, Harris NL. Osteochondral autotransfer—newer treatment for chondral defects. *AORN J*. 2000; 71(4):843. [PubMed: 10806538]
7. Curl WW, Krome J, Gordon ES, et al. Cartilage injuries: a review of 31,516 knee arthroscopies. *Arthroscopy*. 1997; 13(4):456. [PubMed: 9276052]
8. Lattermann C, Kang RW, Cole BJ. What's new in the treatment of focal chondral defects of the knee? *Orthopedics*. 2006; 29(10):898. [PubMed: 17061416]
9. Zeni JA Jr, Axe MJ, Snyder-Mackler L. Clinical predictors of elective total joint replacement in persons with end-stage knee osteoarthritis. *BMC Musculoskelet Disord*. 2010; 11:86. [PubMed: 20459622]
10. Ranawat CS, Flynn WF Jr, Saddler S, et al. Long-term results of the total condylar knee arthroplasty. A 15-year survivorship study. *Clin Orthop Relat Res*. 1993; 286:94. [PubMed: 8425373]
11. Rand JA, Ilstrup DM. Survivorship analysis of total knee arthroplasty. Cumulative rates of survival of 9200 total knee arthroplasties. *J Bone Joint Surg Am*. 1991; 73(3):397. [PubMed: 2002078]

12. Kurtz SM, Lau E, Ong K, et al. Future young patient demand for primary and revision joint replacement: national projections from 2010 to 2030. *Clin Orthop Relat Res*. 2009; 467(10):2606. [PubMed: 19360453]
13. Sinha, RK. Revision total knee arthroplasty.. In: Fitzgerald, RH.; Kaufer, H.; Malkani, AL., editors. *Orthopaedics*. Mosby; St. Louis: 2002. p. 100
14. Crowder AR, Duffy GP, Trousdale RT. Long-term results of total knee arthroplasty in young patients with rheumatoid arthritis. *J Arthroplasty*. 2005; 20(7 Suppl 3):12. [PubMed: 16213997]
15. Dahm DL, Barnes SA, Harrington JR, et al. Patient-reported activity level after total knee arthroplasty. *J Arthroplasty*. 2008; 23(3):401. [PubMed: 18358379]
16. O'Driscoll SW. The healing and regeneration of articular cartilage. *J Bone Joint Surg Am*. 1998; 80(12):1795. [PubMed: 9875939]
17. W-Dahl A, Robertsson O, Lidgren L. Surgery for knee osteoarthritis in younger patients. *Acta Orthop*. 2010; 81(2):161. [PubMed: 19968599]
18. Diduch DR, Insall JN, Scott WN, et al. Total knee replacement in young, active patients. Long-term follow-up and functional outcome. *J Bone Joint Surg Am*. 1997; 79(4):575. [PubMed: 9111404]
19. Bisschop R, Brouwer RW, Van Raay JJ. Total knee arthroplasty in younger patients: a 13-year follow-up study. *Orthopedics*. 2010; 33(12):876. [PubMed: 21162506]
20. Jackson M, Sarangi PP, Newman JH. Revision total knee arthroplasty. Comparison of outcome following primary proximal tibial osteotomy or unicompartmental arthroplasty. *J Arthroplasty*. 1994; 9(5):539. [PubMed: 7807113]
21. Bono, JV.; Scott, RD. *Revision total knee arthroplasty*. Springer; New York, NY: 2005.
22. Goldberg VM, Figgie MP, Figgie HE III, et al. The results of revision total knee arthroplasty. *Clin Orthop Relat Res*. 1988; 226:86. [PubMed: 3335110]
23. Shannon BD, Klassen JF, Rand JA, et al. Revision total knee arthroplasty with cemented components and uncemented intramedullary stems. *J Arthroplasty*. 2003; 18(7 Suppl 1):27. [PubMed: 14560407]
24. Deirmengian CA, Lonner JH. What's new in adult reconstructive knee surgery. *J Bone Joint Surg Am*. 2009; 91(12):3008. [PubMed: 19952268]
25. Gill TJ. The treatment of articular cartilage defects using microfracture and debridement. *Am J Knee Surg*. 2000; 13(1):33. [PubMed: 11826923]
26. Kreuz PC, Steinwachs MR, Erggelet C, et al. Results after microfracture of full-thickness chondral defects in different compartments in the knee. *Osteoarthritis Cartilage*. 2006; 14(11):1119. [PubMed: 16815714]
27. Smolders JM, Kock NB, Koeter S, et al. Osteochondral autograft transplantation for osteochondritis dissecans of the knee. Preliminary results of a prospective case series. *Acta Orthop Belg*. 76(2):208. [PubMed: 20503947]
28. Hangody L, Feczko P, Bartha L, et al. Mosaicplasty for the treatment of articular defects of the knee and ankle. *Clin Orthop Relat Res*. 2001; 391(Suppl):S328. [PubMed: 11603716]
29. Bedi A, Feeley BT, Williams RJ III. Management of articular cartilage defects of the knee. *J Bone Joint Surg Am*. 2010; 92(4):994. [PubMed: 20360528]
30. Hangody L, Vasarhelyi G, Hangody LR, et al. Autologous osteochondral grafting—technique and long-term results. *Injury*. 2008; 39(Suppl 1):S32. [PubMed: 18313470]
31. McNickle AG, L'Heureux DR, Yanke AB, et al. Outcomes of autologous chondrocyte implantation in a diverse patient population. *Am J Sports Med*. 2009; 37(7):1344. [PubMed: 19286911]
32. Ruano-Ravina A, Jato Diaz M. Autologous chondrocyte implantation: a systematic review. *Osteoarthritis Cartilage*. 2006; 14(1):47. [PubMed: 16242355]
33. Raghunath J, Rollo J, Sales KM, et al. Biomaterials and scaffold design: key to tissue-engineering cartilage. *Biotechnol Appl Biochem*. 2007; 46(Pt 2):73. [PubMed: 17227284]
34. Kawalec JS, Hetherington VJ, Melillo TC, et al. Evaluation of fibrocartilage regeneration and bone response at full-thickness cartilage defects in articulation with pyrolytic carbon or cobalt–chromium alloy hemiarthroplasties. *J Biomed Mater Res*. 1998; 41(4):534. [PubMed: 9697025]

35. Kirker-Head CA, Van Sickle DC, Ek SW, et al. Safety of, and biological and functional response to, a novel metallic implant for the management of focal full-thickness cartilage defects: preliminary assessment in an animal model out to 1 year. *J Orthop Res.* 2006; 24(5):1095. [PubMed: 16609973]
36. Ushio K, Oka M, Hyon SH, et al. Partial hemiarthroplasty for the treatment of osteonecrosis of the femoral head. An experimental study in the dog. *J Bone Joint Surg Br.* 2003; 85(6):922. [PubMed: 12931820]
37. Custers RJ, Saris DB, Dhert WJ, et al. Articular cartilage degeneration following the treatment of focal cartilage defects with ceramic metal implants and compared with microfracture. *J Bone Joint Surg Am.* 2009; 91(4):900. [PubMed: 19339575]
38. Guldberg RE, Richards M, Caldwell NJ, et al. Trabecular bone adaptation to variations in porous-coated implant topology. *J Biomech.* 1997; 30(2):147. [PubMed: 9001935]
39. Bobyn JD, Pilliar RM, Cameron HU, et al. The optimum pore size for the fixation of porous-surfaced metal implants by the ingrowth of bone. *Clin Orthop Relat Res.* 1980; 150:263. [PubMed: 7428231]
40. Collins, D. *The pathology of articular and spinal diseases.* Edward Arnold; London: 1949.
41. Mankin HJ, Dorfman H, Lippiello L, et al. Biochemical and metabolic abnormalities in articular cartilage from osteo-arthritic human hips. II. Correlation of morphology with biochemical and metabolic data. *J Bone Joint Surg Am.* 1971; 53(3):523. [PubMed: 5580011]
42. van der Sluijs JA, Geesink RG, van der Linden AJ, et al. The reliability of the Mankin score for osteoarthritis. *J Orthop Res.* 1992; 10(1):58. [PubMed: 1727936]
43. Chevalier J, Gremillard L, Deville S. Low-temperature degradation of zirconia and implications for biomedical implants. *Annu Rev Mater Res.* 2007; 37:1.
44. ISO. *Implants for surgery — ceramic materials based on yttria-stabilized tetragonal zirconia (Y-TZP).* International Organization for Standardization; 2008.
45. Ghadially JA, Ghadially FN. Evidence of cartilage flow in deep defects in articular cartilage. *Virchows Arch B Cell Pathol.* 1975; 18(3):193. [PubMed: 808028]
46. Ghadially FN, Thomas I, Oryschak AF, et al. Long-term results of superficial defects in articular cartilage: a scanning electron-microscope study. *J Pathol.* 1977; 121(4):213. [PubMed: 874638]
47. Ghadially JA, Ghadially R, Ghadially FN. Long-term results of deep defects in articular cartilage. A scanning electron microscope study. *Virchows Arch B Cell Pathol.* 1977; 25(2):125. [PubMed: 412310]
48. Bauer MS, Woodard JC, Weigel JP. Effects of exposure to ambient air on articular cartilage of rabbits. *Am J Vet Res.* 1986; 47(6):1268. [PubMed: 3729126]
49. Speer KP, Callaghan JJ, Seaber AV, et al. The effects of exposure of articular cartilage to air. A histochemical and ultrastructural investigation. *J Bone Joint Surg Am.* 1990; 72(10):1442. [PubMed: 2254350]



Fig. 1. Ceramic implant device is monolithic in form, with a highly polished submicron articular surface (top) and two interconnected porous cones exhibiting approximately 60% porosity (patents pending).

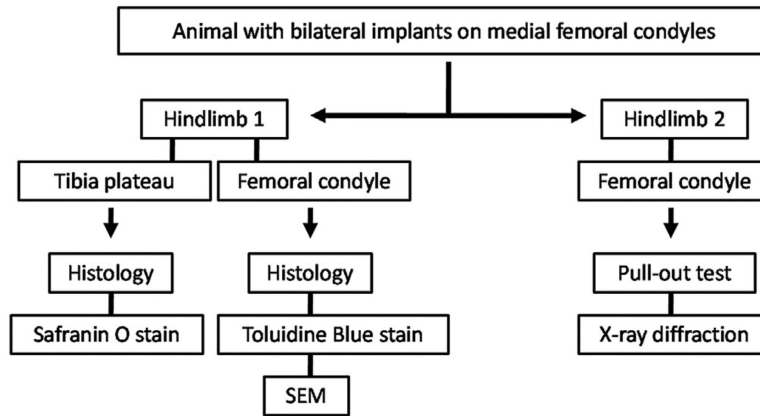


Fig. 2.
Experimental outcomes flowchart.

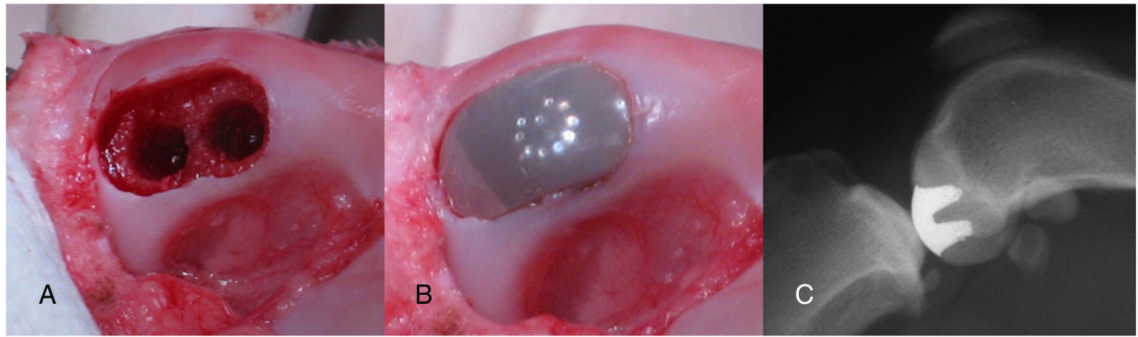


Fig. 3. Surgical procedure and postoperative radiograph. (A) Insertion site. (B) Inserted implant. (C) Representative lateral knee radiograph.

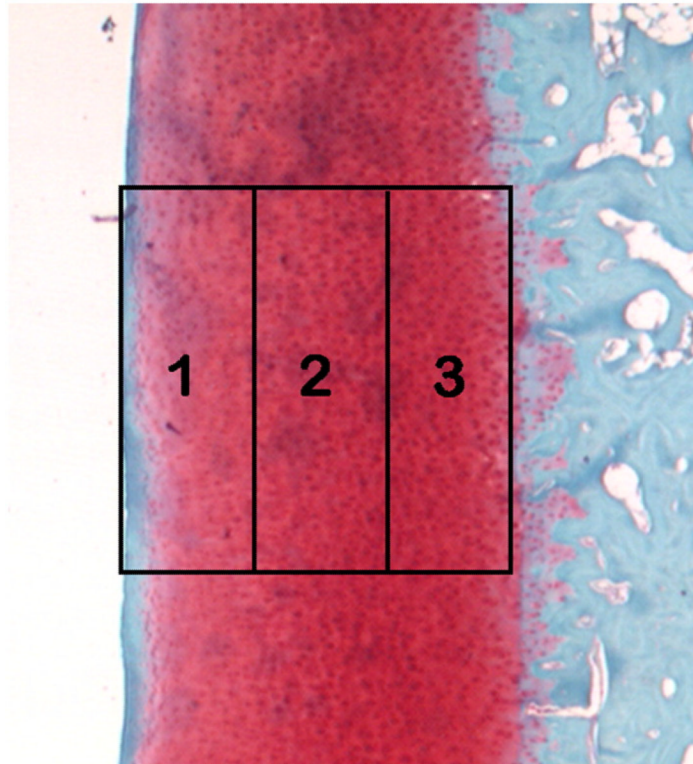


Fig. 4. Safranin O-stained articular cartilage from tibial plateau with regions shown. The articular surface is represented by region 1, while region 3 is closest to the subchondral bone.

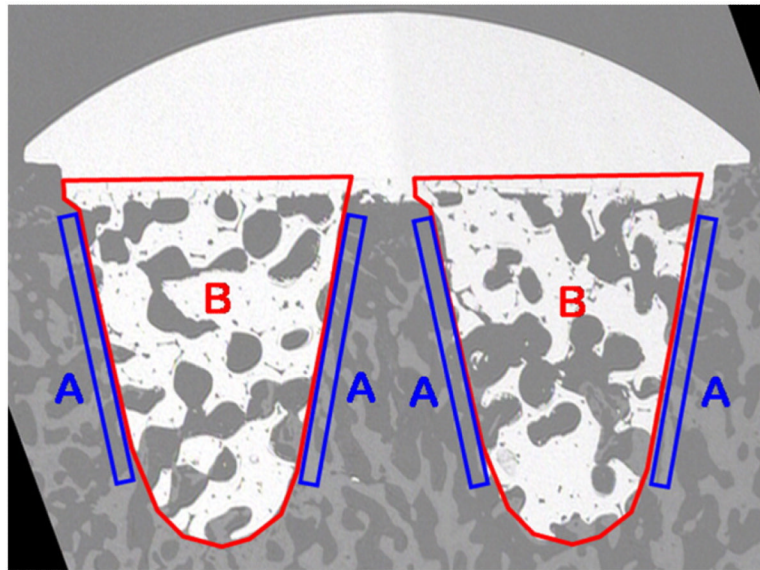


Fig. 5. Scanning electron microscopy images of center section of implant. Apposition and bone ingrowth regions are labeled “A” and “B”, respectively.

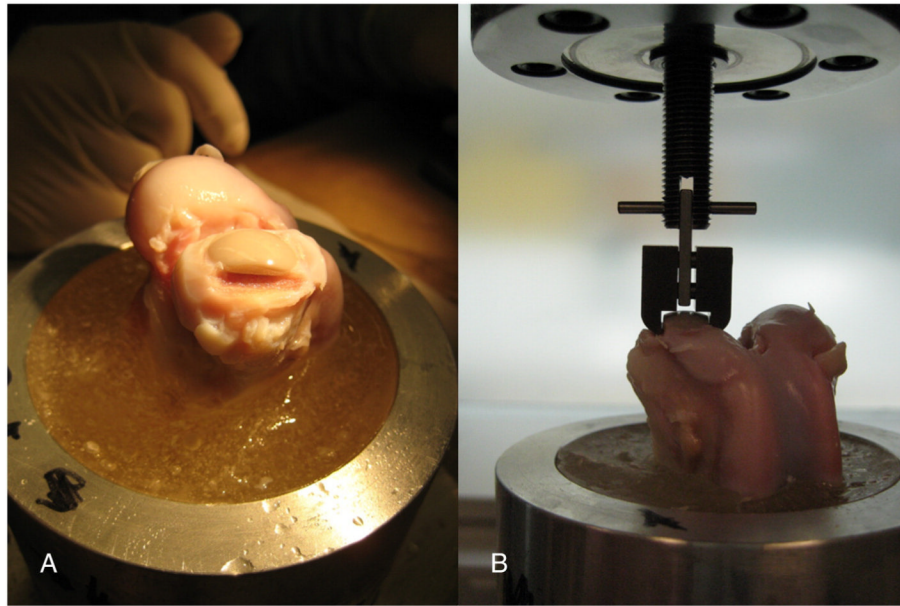


Fig. 6. Pull-out test. (A) PMMA-embedded distal femur with implant in medial condyle, with cartilage immediately medial and lateral to the implant removed to ensure custom clamp fit. (B) Vertical alignment of specimen in servohydraulic testing machine using a multidirectional vice.

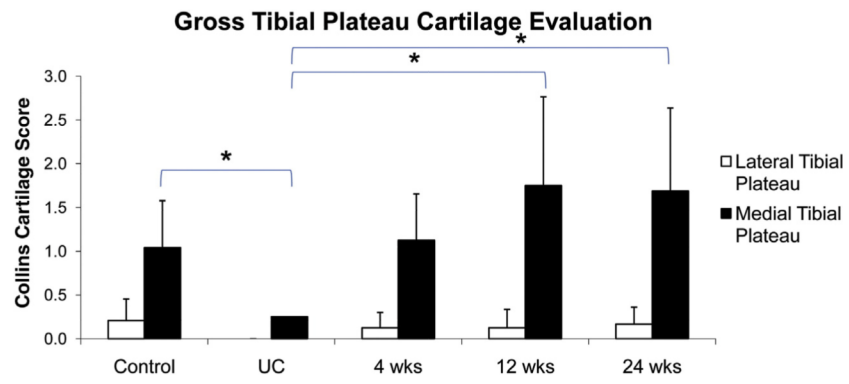


Fig. 7. Gross cartilage evaluation of tibial plateau upon dissection. Two independent reviewers performed the evaluation using the Collins score.

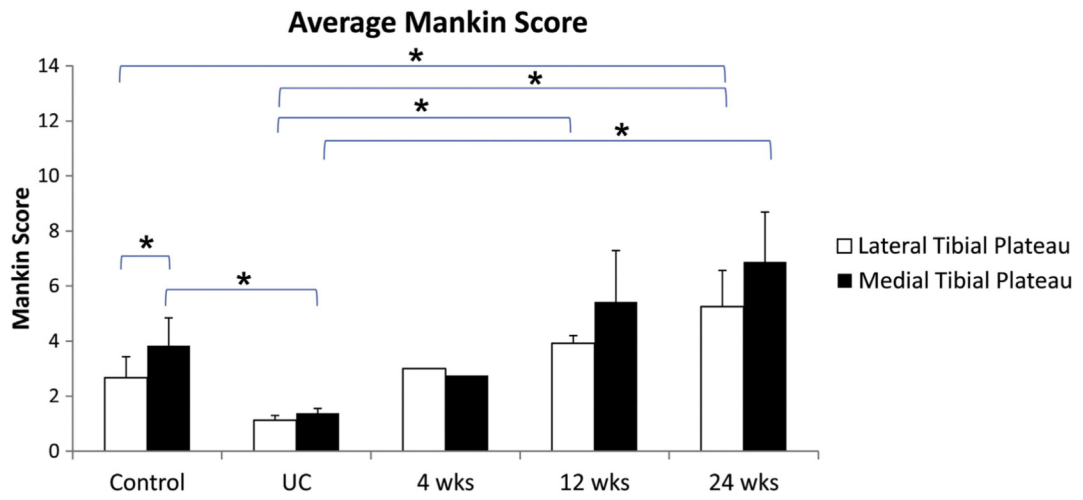


Fig. 8. Evaluation of Safranin O-stained sections of tibial plateau cartilage. Two independent reviewers scored the articular cartilage using the 14-point Mankin score.

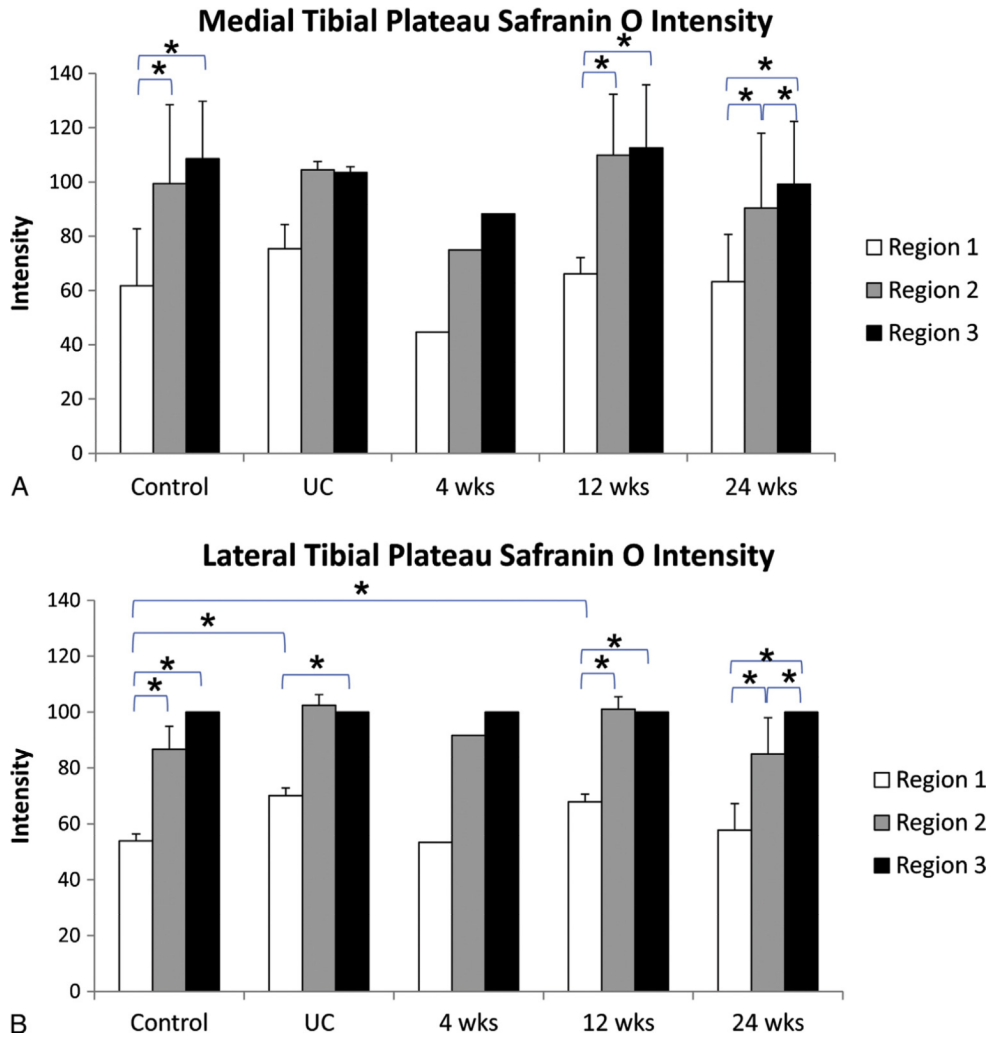


Fig. 9. Tibial plateau Safranin O intensity. Intensities are relative to the intensity of the region closest to the subchondral bone (region 3) on the lateral plateau within each animal. (A) Medial tibial plateau Safranin O intensity. (B) Lateral tibial plateau Safranin O intensity.

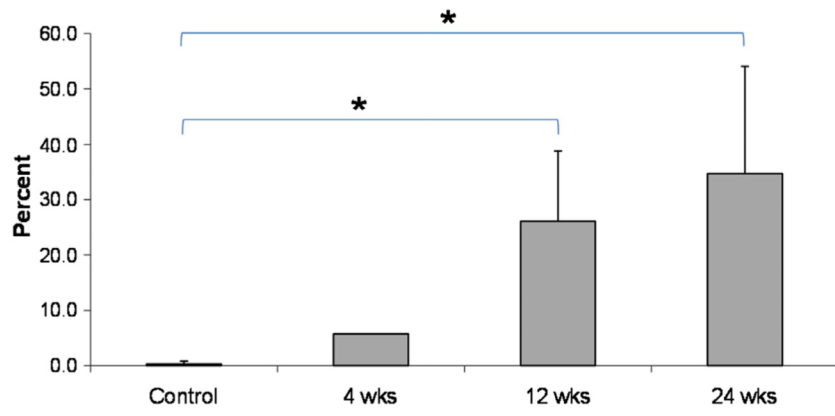


Fig. 10. Percent implant articular surface length (IASL) covered by cartilage.

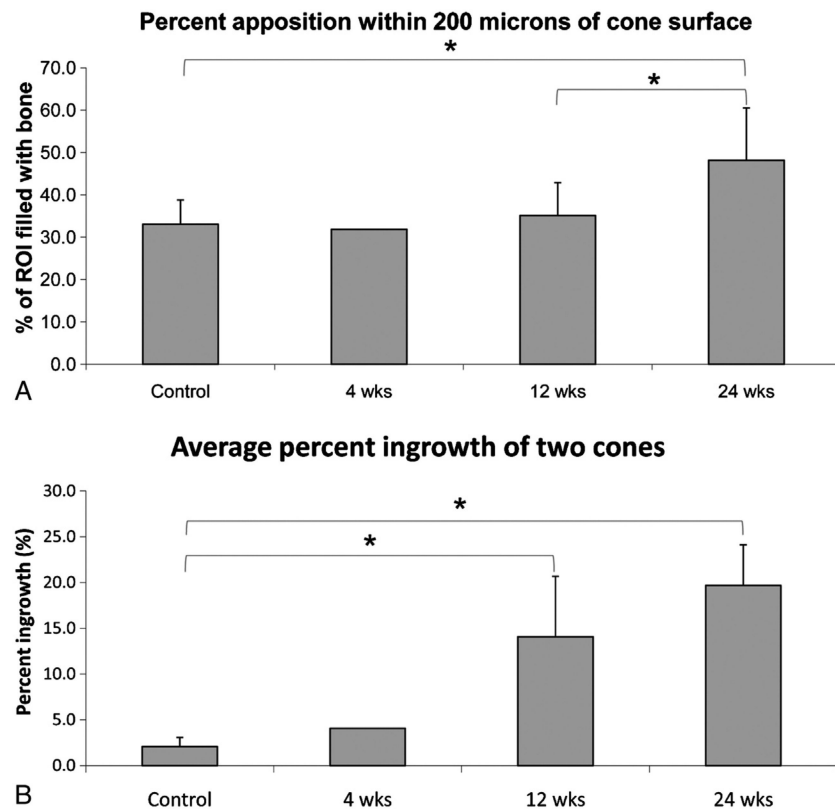


Fig. 11. Scanning electron microscopy analysis of bone apposition and bone ingrowth of implant. (A) Percent bone apposition within 200 μm of the cone surface. (B) Average percent ingrowth of the two cones within each implant.

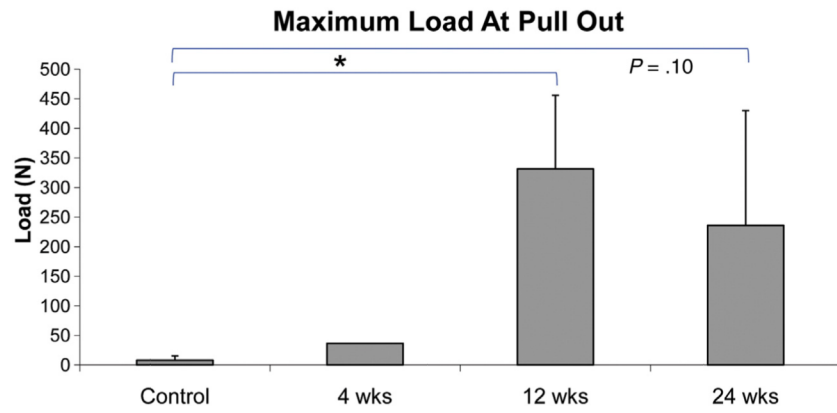


Fig. 12. Maximum load during unidirectional biomechanical pull-out test of implants.

Table 1

Ceramic Stability (Monoclinic Phase Transformation Percentage) on Non-Implanted and Implanted Devices.

Specimen	Specimen History	Analysis Location	No. of Specimens	% Monoclinic Phase
Implant	Not Implanted	Articular Surface	3	<1%
Implant	Not Implanted	Scaffold Surface	3	<1%
Implant	Implanted 4 weeks	Articular Surface	1	<1%
Implant	Implanted 12 weeks	Articular Surface	1	<1%
Implant	Implanted 24 weeks	Articular Surface	2	<2%
Implant	Implanted 4 weeks	Scaffold Surface	1	<1%
Implant	Implanted 12 weeks	Scaffold Surface	1	<1%
Implant	Implanted 24 weeks	Scaffold Surface	2	<3%